

## Nonprecious Metal Borides: Emerging Electrocatalysts for Hydrogen Production

Eunsoo Lee and Boniface P. T. Fokwa\*



Cite This: *Acc. Chem. Res.* 2022, 55, 56–64



Read Online

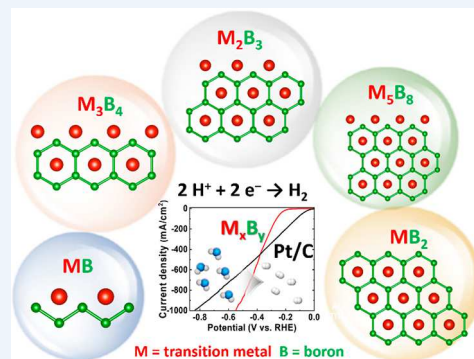
ACCESS |

Metrics & More

Article Recommendations

**CONSPICUOUS:** The development of highly active noble-metal-free catalysts for the hydrogen evolution reaction (HER) is the focus of current fundamental research, aiming for a more efficient and economically affordable water-splitting process. While most HER catalysts are studied only at the nanoscale (small particle size and high surface area), metal borides (MBs) are mostly studied in bulk form. This offers a unique opportunity for designing highly efficient and nonprecious HER MBs electrocatalysts based on structure–activity relationships, especially because of their rich compositional and structural diversity.

In this Account, we focus on the importance of boron and its substructures in achieving extraordinary HER performances and the importance of using structure–activity relationships to design next-generation MBs electrocatalysts. Studying the Mo–B system, we found that the HER activity of molybdenum borides increases with increasing boron content: from Mo<sub>2</sub>B (no B–B bonds in the structure, least active) to α-MoB and β-MoB (zigzag boron chains, intermediate activity) and MoB<sub>2</sub> (planar graphene-like boron layer, most active). Density functional theory (DFT) calculations have shown that the (001) boron layer in hexagonal MoB<sub>2</sub> (α-MoB<sub>2</sub>) is the most active surface and has similar HER activity behavior like the benchmark Pt(111) surface. However, puckering this flat boron layer to the chair-like configuration (phosphorene-like layer) drastically reduces its activity, thereby making the rhombohedral modification of MoB<sub>2</sub> (Mo<sub>2</sub>B<sub>4</sub> or β-MoB<sub>2</sub>) less active than α-MoB<sub>2</sub>. This discovery was then further supported by studies of the Mo–W–B system. In fact, the binary WB<sub>2</sub>, which also contains the puckered boron layer, is also less active than α-MoB<sub>2</sub>, despite containing the more active transition metal W, which performs better in elemental form than Mo. To design a superior catalyst, the more active W was then stabilized in the hexagonal α-MoB<sub>2</sub> structure through the synthesis of α-Mo<sub>0.7</sub>W<sub>0.3</sub>B<sub>2</sub>, which indeed proved to be a better HER electrocatalyst than α-MoB<sub>2</sub>. Using the isoelectronic Cr instead of W led to the α-Cr<sub>1-x</sub>Mo<sub>x</sub>B<sub>2</sub> solid solution, the HER activity of which followed unexpected canonic-like (or volcano-like) behavior that perfectly matched that of the *c* lattice parameter trend, thereby producing the best catalyst α-Cr<sub>0.4</sub>Mo<sub>0.6</sub>B<sub>2</sub> that outperformed Pt/C at high current density, thus underscoring the effectiveness of the structure–activity concept in designing highly active catalysts. This concept was further applied to the V–B system, leading to the discovery of an unexpected boron chain dependency of the HER activity that ultimately led to the prediction of new V<sub>x</sub>B<sub>y</sub> catalysts and their crystal structures and overpotentials. Finally, reducing the particle sizes of all of these bulk crystalline catalysts is also possible and offers an even greater potential as demonstrated for nanoscale α-MoB<sub>2</sub> and VB<sub>2</sub>. Nevertheless, these crystalline nanomaterials are still highly agglomerated due to the high temperature required for their synthesis, thus the synthesis of highly dispersed MBs is an urgent goal that will enable the fulfillment of their extraordinary potential in the future.



### KEY REFERENCES

- Park, H.; Encinas, A.; Scheifers, J. P.; Zhang, Y.; Fokwa, B. P. T. Boron-dependency of molybdenum boride electrocatalysts for the hydrogen evolution reaction. *Angew. Chem., Int. Ed.* 2017, 56, 5575–5578.<sup>1</sup> Binary polycrystalline molybdenum borides (Mo<sub>2</sub>B, α-MoB, β-MoB, and MoB<sub>2</sub>) have been successfully synthesized, and their HER activities have been reported. The HER activity increases with increasing boron content, indicating a strong boron dependency of these borides for the HER.
- Park, H.; Zhang, Y.; Scheifers, J. P.; Jothi, P. R.; Encinas, A.; Fokwa, B. P. T. Graphene- and phosphorene-like

boron layers with contrasting activities in highly active Mo<sub>2</sub>B<sub>4</sub> for hydrogen evolution. *J. Am. Chem. Soc.* 2017, 139, 12915–12918.<sup>2</sup> Mo<sub>2</sub>B<sub>4</sub> (or β-MoB<sub>2</sub>), which contains both graphene-like and phosphorene-like B layers, has been synthesized by the tin flux method. ΔG<sub>H</sub> calculations show

Received: August 30, 2021

Published: December 14, 2021



that the graphene-like B layer is far more HER active than the phosphorene-like B layer, supporting the experimental finding that  $\beta$ -MoB<sub>2</sub> is less active than  $\alpha$ -MoB<sub>2</sub>.

- Park, H.; Lee, E.; Lei, M.; Joo, H.; Coh, S.; Fokwa, B. P. T. Canonic-Like HER Activity of Cr<sub>1-x</sub>Mo<sub>x</sub>B<sub>2</sub> Solid Solution: Overpowering Pt/C at High Current Density. *Adv. Mater.* **2020**, *32*, 2000855.<sup>3</sup> Unusual canonic-like (or volcano-like) behavior of the c-lattice parameter in Cr<sub>1-x</sub>Mo<sub>x</sub>B<sub>2</sub> and its direct correlation to the HER activity are reported. DFT calculations reproduced the behavior of the c-lattice parameter and demonstrated that the (110) layer promotes HER more efficiently for  $x = 0.6$ , the most-HER-active composition.
- Lee, E.; Park, H.; Joo, H.; Fokwa, B. P. T. Unexpected Correlation Between Boron Chain Condensation and HER Activity in Highly Active Vanadium Borides: Enabling Predictions. *Angew. Chem., Int. Ed.* **2020**, *59*, 11774–11778.<sup>4</sup> The high activity of V<sub>x</sub>B<sub>y</sub> has been rationalized by studying the effect of aggregating boron chains as a function of HER activity. A structure–activity relationship is found that helps to predict new phases and their HER overpotentials.

## ■ INTRODUCTION

Metal borides (MBs) constitute a class of materials that are still exotic to most chemists and material scientists, despite some excellent properties that have led to many industrial applications such as permanent magnets (Nd<sub>2</sub>Fe<sub>14</sub>B), superconductors (MgB<sub>2</sub>), and bulk refractory and conductive ceramics (ZrB<sub>2</sub>, HfB<sub>2</sub>), just to name a few.<sup>5,6</sup> Structurally, metal borides can be divided into three groups depending on their relative boron content and the types of bonds that characterize each group. The first group concerns boron-rich borides and has a small metal-to-boron ratio ( $M/B < 0.5$ ), with the highest boron content found in the YB<sub>66</sub> phase, which is an exciting phase used as a monochromator for synchrotron radiation. These boron-rich borides are structurally characterized by the presence of three-dimensional (3D) boron networks and have no metal–metal bonds. The second group concerns metal-rich borides ( $M/B > 2$ ), with permanent magnet Nd<sub>2</sub>Fe<sub>14</sub>B being one of the metal-richest compositions. In contrast to the previous group, here the 3D network is built by the metal atoms and therefore there are no boron–boron bonds. The third group comprises borides with moderate boron content ( $0.5 \leq M/B \leq 2$ ), the structures of which mostly contain all possible bonds. However, the boron atoms in this group usually build low-dimensional substructures (boron dumbbells, boron chains, and boron layers).<sup>5–7</sup>

Some exciting properties of bulk metal borides have been the focus of recent investigations, including superhardness, thermoelectric, and magnetic properties.<sup>5,8</sup> In particular, transition-metal borides have attracted considerable attention as catalytic and battery materials because they are easy to synthesize on a large scale and are inexpensive.<sup>8</sup> Therefore, unlike precious metals, large-scale applications are possible. For example, nickel boride (NiB) and cobalt boride (CoB) are being explored as catalysts for the hydrodesulfurization reaction.<sup>9</sup> Furthermore, TiB<sub>2</sub>, VB<sub>2</sub>, FeB, and CoB are considered to be multielectron-transfer anode materials for high-energy-density batteries.<sup>10</sup> Also, it was shown that PtB clusters (subnanoscale) supported on alumina have improved selectivity in dehydrogenation if compared to boron-less Pt

clusters.<sup>11</sup> Recently, crystalline metal borides have attracted attention as active catalysts for oxidative dehydrogenation and nitrogen reduction reactions.<sup>12,13</sup> However, MBs as electrocatalysts for the hydrogen evolution reaction (HER) and the oxygen evolution reaction (OER) have seen the most interest, as demonstrated by three recent reviews of these rapidly evolving research areas.<sup>14–16</sup> Initially, the MBs studied as HER electrocatalysts were mostly amorphous.<sup>17–19</sup> However, bulk and nanoscale crystalline MBs have seen a rapid rise in recent years. For example, the crystalline FeB<sub>2</sub>, RuB, and VB<sub>2</sub> nanomaterials are found to be even better HER electrocatalysts than the nanoscale amorphous binary borides.<sup>20–22</sup> Nanoscale RuB<sub>2</sub> is reported to have activity similar to that of the benchmark Pt/C in acidic solution and performs better than Pt/C in alkaline solution, but it still contains the precious Ru metal.<sup>23</sup> Despite the recent success as demonstrated in these newly published reviews,<sup>14–16</sup> if compared to sulfides, carbides, or phosphides, which are considered for similar applications and are mostly studied at the nanoscale,<sup>24</sup> metal borides are far from being extensively explored, owing mainly to the difficulties encountered during their nanoscale synthesis.<sup>25</sup>

Conventionally, metal borides have been synthesized from the direct combination of a metal with boron at high temperatures and/or high pressures (for example, by arc melting above 2500 °C), the reduction of a metal oxide or salts with boron compounds such as alkali borohydrides (NaBH<sub>4</sub>), boron oxide (B<sub>2</sub>O<sub>3</sub>), and dehydrated borax (Na<sub>2</sub>B<sub>4</sub>O<sub>7</sub>) in a molten metal, the reaction of a boron halide with a metal or metal oxide and hydrogen, and fused salt electrolysis of a metal oxide with boron oxide.<sup>25</sup> For large-scale preparation, borides are typically made from a carbothermal reduction of metal oxides using B<sub>2</sub>O<sub>3</sub> or B<sub>4</sub>C and carbon at temperatures above 1400 °C, followed by high-temperature purification techniques. The high-temperature synthesis undoubtedly leads to large particle sizes, uncontrolled crystallization, and mixed-phase products. As an example, even the commercially available crystalline  $\alpha$ -MoB is still contaminated by  $\beta$ -MoB.<sup>26</sup> At the nanoscale, the situation is even worse because the stabilization of the complex bonding patterns (often a mixture of strongly covalent and metallic bonds) found in these materials usually requires high temperatures, leading to severe particle agglomeration that is detrimental to catalytic activity.<sup>25</sup>

As mentioned above, the challenges encountered during the synthesis of nanocrystalline MBs had initially led to the HER studies of amorphous nanoscale metal borides instead.<sup>17–19</sup> While such research is important and can even lead to useful applications, it is inadequate for structure–activity relationship studies because of the lack of long-range ordering and (in some cases) the lack of precise compositions. Interestingly, the high HER activity of nanocrystalline MBs, despite their high particle agglomeration, is due to the fact that these materials are already highly active in the bulk, a discovery made in 2012 by Vruble and Hu.<sup>26</sup> Consequently, the structure–activity relationships can be leveraged in MBs by taking advantage of their extraordinary structural and compositional diversity coupled to their excellent HER activity in the bulk. We initiated this route in 2017, and recent developments focusing on nonprecious metal borides are summarized below.

## ■ BORON DEPENDENCY OF HER ACTIVITY IN METAL BORIDES

Vruble and Hu first found in 2012 that the commercially available polycrystalline molybdenum boride,  $\alpha$ -MoB (particle

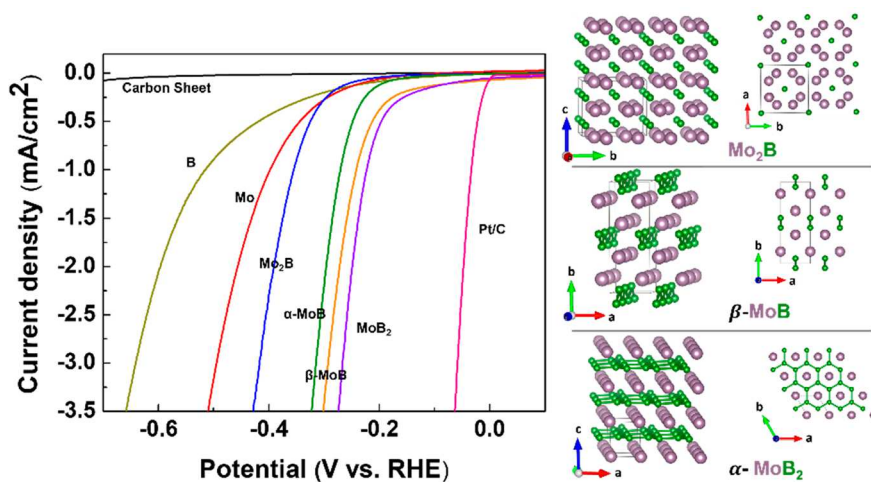


**Figure 1.** (Left) Polarization curves for amorphous B, Mo, Mo<sub>2</sub>B,  $\alpha$ -MoB,  $\beta$ -MoB, and  $\alpha$ -MoB<sub>2</sub> measured in 0.5 M H<sub>2</sub>SO<sub>4</sub>. IR-drop was corrected. (Right) crystal structures of Mo<sub>2</sub>B,  $\beta$ -MoB, and  $\alpha$ -MoB<sub>2</sub>. Adapted with permission from ref 1. Copyright 2017 Wiley.

size 1–3  $\mu\text{m}$ , CrB-type structure), exhibited excellent HER activity in both acidic and basic solutions and showed a 100% Faradaic yield for hydrogen evolution.<sup>26</sup> Furthermore, they found that the oxides present on the surface of the material, MoO<sub>2</sub> and MoO<sub>3</sub>, as well as Mo metal are not efficient catalysts for HER and that the oxides dissolved in the acid electrolyte after activation according to the XPS measurements.<sup>26</sup> This finding suggested that the HER activity was due to the surface boride and not the oxide. Our first contribution to this field was aimed at (1) finding out if the other MoB polymorph,  $\beta$ -MoB (MoB-type), was as active as  $\alpha$ -MoB, (2) studying the HER activity of other phases in the Mo–B system, and (3) finding out if a structure–activity relationship could be derived in the Mo–B system. Therefore, we synthesized, by arc-melting, four binary bulk molybdenum borides, Mo<sub>2</sub>B,  $\alpha$ -MoB,  $\beta$ -MoB, and  $\alpha$ -MoB<sub>2</sub>, and studied their HER activities in acidic electrolyte, in comparison with elemental Mo and B.<sup>1</sup> We found that Mo and B are noncompetitive HER catalysts, but Mo is more active than B because Mo is metallic while B is semiconducting. Surprisingly, when Mo and B form compounds, the HER activity increases (overpotential decreases) with increasing boron content (Figure 1, left), indicating that boron is playing a crucial role. In particular, the presence of boron–boron bonds (Figure 1, right) favors HER activity: while  $\alpha$ -Mo<sub>2</sub>B (no B–B bonds) is a less-active HER catalyst,  $\alpha$ -MoB,  $\beta$ -MoB, and  $\alpha$ -MoB<sub>2</sub> are highly active, with hexagonal  $\alpha$ -MoB<sub>2</sub> (AlB<sub>2</sub>-type structure) being the best. This discovery has since enabled the study of other boride systems such as W–B and Ru–B by other research groups who found the same trend in higher HER activity for the MB<sub>2</sub> (M = W, Ru) diborides.<sup>21,27</sup> Interestingly, the crystal structures of diborides  $\alpha$ -MoB<sub>2</sub>, WB<sub>2</sub>, and RuB<sub>2</sub> are all different, but they differ mainly by their B substructure, which is a planar graphene-like B layer in  $\alpha$ -MoB<sub>2</sub>, a 50:50 mixture of planar and chair-like puckered B layers in WB<sub>2</sub> and a boat-like puckered B layer in RuB<sub>2</sub>.<sup>5,6</sup> While the remarkably high Pt/C-like HER activity of RuB<sub>2</sub> can be attributed to the additional contribution of the highly active platinum group and precious element Ru, the high HER activities of  $\alpha$ -MoB<sub>2</sub> and WB<sub>2</sub> originate mainly from the B substructure because the W and Mo elements are not as HER active as Ru. This in turn

raises the question of the role of the type of B-layer conformation in the different activities of these diborides.

Density functional theory (DFT) calculations, specifically the Gibbs free energy ( $\Delta G_{\text{H}}$ ) of H adsorption, were performed on different surfaces of  $\alpha$ -MoB<sub>2</sub> as well as the (111) layer of Pt and the (110) layer of elemental Mo (for comparison) to understand the origin of the high HER activity of this boride phase.<sup>28</sup> Optimal activity is achieved at a  $\Delta G_{\text{H}}$  value close to zero, where the overall reaction of both H adsorption and H<sub>2</sub> desorption has the maximum rate.<sup>29</sup> The results showed that boron is indeed playing a prominent role in the catalytic activity of  $\alpha$ -MoB<sub>2</sub>: in fact, the graphene-like B (001) layer has HER activity behavior similar to that of the benchmark Pt (111) layer (compare black and dashed red lines in Figure 2).<sup>28</sup> Specifically, with increasing H coverage  $\Delta G_{\text{H}}$  increases in

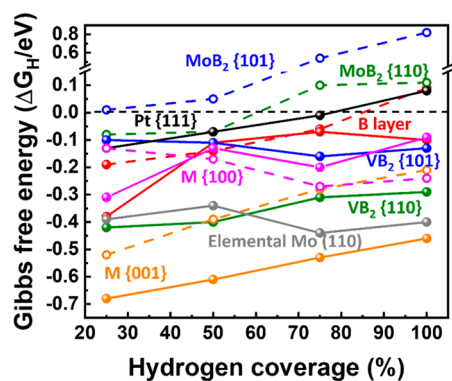


**Figure 2.** Gibbs free energy ( $\Delta G_{\text{H}}$ ) for H adsorption on the surfaces of Pt, elemental Mo, and  $\alpha$ -MoB<sub>2</sub> plotted as a function of hydrogen coverage. Gibbs free energy ( $\Delta G_{\text{H}}$ ) for H adsorption on the surfaces of {111} Pt (black), elemental {001} Mo (gray), and multiple surfaces for MoB<sub>2</sub> (dashed lines) and VB<sub>2</sub> (solid lines) plotted as a function of hydrogen coverage. {hkl} represents a set of (hkl) planes.

both cases and reaches zero at high H coverages. However, the Mo (001) and (100) layers were far less active as their  $\Delta G_{\text{H}}$  curves never reached zero. However, they perform better than elemental Mo (110) at high H coverages. Interestingly, the other identified highly active surface, the Mo/B (110) layer also contains boron, further confirming the importance of



boron in the HER activity of this phase. Consequently, multiple B-containing surfaces are active in this phase, which may explain the high HER activity of bulk borides. Nevertheless, the most active surface is the graphene-like boron layer, a discovery which suggested that  $AlB_2$ -type borides can be an ideal playground for discovering highly active HER electrocatalysts. The viability of this approach was confirmed by a different research group which found that nanocrystalline  $\alpha$ - $FeB_2$  is highly active mainly because of its flat boron layer.<sup>20</sup> Our subsequent DFT calculations showed that puckering the flat boron layer to the chair-like conformation (phosphorene-like layer, Figure 3) drastically reduces its activity. Con-

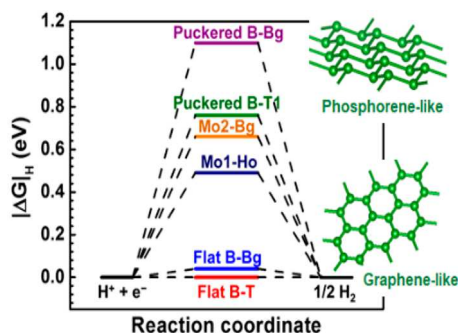


**Figure 3.** Calculated Gibbs free energy diagram for HER over different surfaces at 50% H coverage in  $\beta$ - $MoB_2$ . (Right) Substructures of the two types of boron layers present in  $\beta$ - $MoB_2$ . Reproduced with permission from ref 2. Copyright 2017 American Chemical Society.

sequently, the rhombohedral modification of  $MoB_2$  ( $\beta$ - $MoB_2$ , also known as  $Mo_2B_4$ ) that contains both boron layer types was predicted to be less active than its hexagonal variant,  $\alpha$ - $MoB_2$ , a finding confirmed experimentally (Figure 4).<sup>2</sup> This

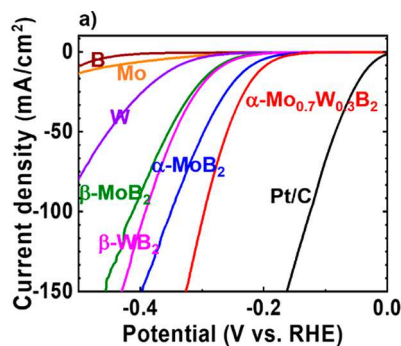


**Figure 4.** Polarization curves for  $\beta$ - $MoB_2$ ,  $\alpha$ - $MoB_2$ ,  $WB_2$ ,  $\alpha$ - $Mo_{0.7}Mo_{0.3}B_2$ , and Pt/C measured in 0.5 M  $H_2SO_4$ . The IR drop was corrected. Reproduced with permission from ref 30. Copyright 2019 Wiley.

result was further supported by the study by us and others of  $WB_2$ , which has an overpotential value closer to that of  $\beta$ - $MoB_2$  than  $\alpha$ - $MoB_2$  (Figure 4).<sup>27,30</sup> Moreover, the lower activity of  $WB_2$  can be explained by the electrochemically active surface area (ECSA). ECSA was estimated from the double-layer capacitance ( $C_{dl}$ ), which can be obtained via cyclic voltammetry (CV) measurements. CV was performed in the nonFaradaic potential range with various scan rates, and the difference in current density variation is plotted against scan rate.  $C_{dl}$  is obtained from half the slope of this linear plot.<sup>31</sup>

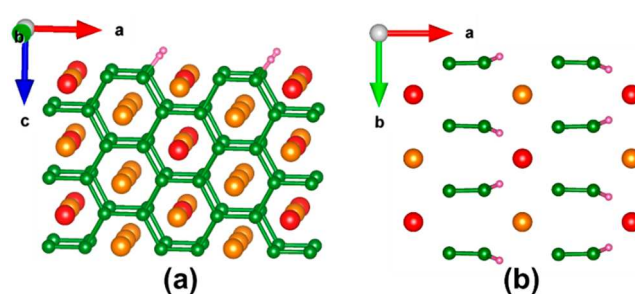


**Figure 5.** (a) Optimized structural configuration on the mixed Mo/W/B (110) surface of  $\alpha$ - $Mo_{0.75}W_{0.25}B_2$  at 100% H coverage. (b) *ab*-plane projection of the 100% H-coverage configuration on the mixed Mo/W/B (110). Mo, W, B, and H atoms are indicated by orange, red, green, and pink spheres, respectively. Reproduced with permission from ref 30. Copyright 2019 Wiley.

The calculated  $C_{dl}$  values of  $\alpha$ - $MoB_2$  and  $WB_2$  (2.3 and 1.6  $mF/cm^2$ , respectively) confirm the above finding. These results show that despite the higher HER activity of elemental W if compared to elemental Mo,  $WB_2$  still has a lower activity than  $\alpha$ - $MoB_2$ , thereby suggesting that the lower HER activity can indeed be attributed mainly to the presence of the 50% puckered chair-like B layer in  $WB_2$ .

## ■ INCREASING HER ACTIVITY BY SOLID-SOLUTION FORMATION IN $AlB_2$ -TYPE BORIDES

### Complex $Mo_{1-x}W_xB_2$ Solid Solution

By taking advantage of the higher activity of W if compared to Mo, we designed a superior catalyst compared to  $\alpha$ - $MoB_2$  by studying the HER activity of the  $Mo_{1-x}W_xB_2$  solid solution.<sup>30</sup> In this complex solid solution, the following phases are present depending on the value of  $x$ :  $\alpha$ - $MoB_2$  ( $x = 0$ ),  $WB_2$  ( $x = 1$ ), single-phase  $\alpha$ - $Mo_{1-x}W_xB_2$  ( $x \leq 0.3$ ), and mixed ternary phases for  $x > 0.3$  (dominated by the  $WB_2$ -type phase). Out of all of these phases, the lowest overpotential was found for  $\alpha$ - $Mo_{0.7}W_{0.3}B_2$  (Figure 4). The high HER activity of  $\alpha$ - $Mo_{0.7}W_{0.3}B_2$  can be rationalized by the fact that the preferred  $AlB_2$ -type structure is maintained (due to the high Mo content), and a significant amount of the more active W is present. Moreover, the ECSA of  $\alpha$ - $Mo_{0.7}W_{0.3}B_2$  estimated by  $C_{dl}$  was larger than those of other phases in this complex solid solution. Interestingly, at higher W concentrations the activity of the  $Mo_{1-x}W_xB_2$  ( $x > 0.3$ ) solid solution decreases, a behavior ascribed to the presence of the less-active  $WB_2$ -type phase in these samples. This finding perfectly illustrates the importance of maintaining the flat boron layer ( $AlB_2$ -type structure) when incorporating a more active element to boost the HER activity of nonprecious metal diborides. To understand the increased HER activity at high current density (at 150  $mA/cm^2$ ) in  $\alpha$ - $Mo_{0.7}W_{0.3}B_2$ , we examined the optimized structural configurations of H adsorption on the Mo/W/B (110) surface of a model phase  $\alpha$ - $Mo_{0.75}W_{0.25}B_2$  at 100% H coverage. Interestingly, two hydrogen atoms bonded to boron atoms were found to be attracted by W and repelled by Mo on this surface (Figure 5a,b). Consequently, W facilitates the bonding between these nearby H atoms toward producing  $H_2$ , a behavior not found for Mo. Therefore, W is mainly responsible for the increased activity at high current density.<sup>30</sup> This finding suggests W to be an interesting nonprecious element for boosting the high-current-density activity of electrocatalysts in general.

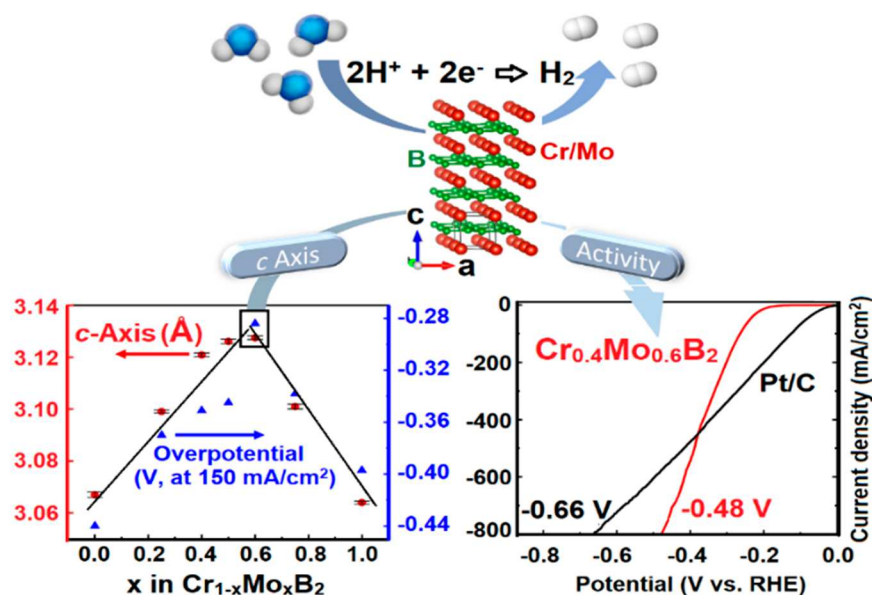


**Figure 6.** (Top) Schematic of HER reaction and crystal structure of  $\alpha\text{-Cr}_{1-x}\text{Mo}_x\text{B}_2$ . (Left) Plots of the *c* lattice parameter and overpotential as a function of *x*. (Right) Polarization curves for  $\alpha\text{-Cr}_{0.4}\text{Mo}_{0.6}\text{B}_2$  and 20% Pt/C measured in 0.5 M  $\text{H}_2\text{SO}_4$ . Reproduced with permission from ref 3. Copyright 2020 Wiley.

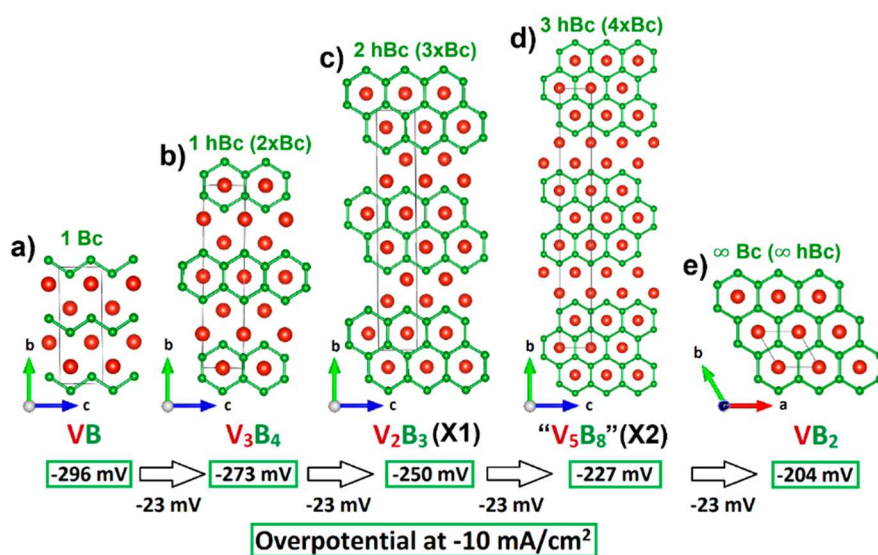


**Figure 7.** Projected crystal structures of known (a) VB, (b)  $\text{V}_3\text{B}_4$ , (c)  $\text{V}_2\text{B}_3$ , and (e)  $\text{VB}_2$  phases. Projected crystal structure of (d) hypothetical  $\text{V}_5\text{B}_8$ . Bc = boron chain; hBc = hexagonal boron chain. Predicted overpotentials (using a  $-23$  mV decrement) for studied and unstudied (X1 and X2) phases. Reproduced with permission from ref 4. Copyright 2020 Wiley.

### Full $\text{Cr}_{1-x}\text{Mo}_x\text{B}_2$ Solid Solution

Building on the design of highly HER-active  $\alpha\text{-Mo}_{0.7}\text{W}_{0.3}\text{B}_2$ , we targeted a 3d transition metal (Cr) and maintained the number of valence electrons to allow for an atomic-size-dependent study within the  $\text{AlB}_2$ -type  $\alpha\text{-Cr}_{1-x}\text{Mo}_x\text{B}_2$  solid solution while lowering the cost of materials.<sup>3</sup> Unlike  $\text{WB}_2$ ,  $\alpha\text{-CrB}_2$  is stable in the  $\text{AlB}_2$ -type structure, enabling the study of the full  $\alpha\text{-Cr}_{1-x}\text{Mo}_x\text{B}_2$  solid solution. The *a*-lattice parameter plot of  $\alpha\text{-Cr}_{1-x}\text{Mo}_x\text{B}_2$  increases linearly with increasing Mo content (*x*) as expected from Vegard's law, but the *c*-lattice parameter plot surprisingly shows canonic-like (or volcano-like) behavior (Figure 6, left) with the maximum at *x* = 0.6. Interestingly, the high-current-density activity (at 150 mA/cm<sup>2</sup>) of this solid solution correlates very well with the canonic-like behavior of

the *c*-lattice parameter plot (Figure 6, left).<sup>3</sup> Furthermore,  $\alpha\text{-Cr}_{0.4}\text{Mo}_{0.6}\text{B}_2$  had the largest  $C_{\text{dl}}$  value of 5.15 mF/cm<sup>2</sup>, which is consistent with the highest HER activity. This is a significant finding because it shows that the variation of a lattice parameter can have a drastic influence on the HER activity of catalysts, thus hinting at the future design of more efficient catalysts by leveraging the structure–activity relationships in borides or in other nonprecious materials. Furthermore, excellent long-term stability and durability were observed for this solid solution, with no significant activity loss after 5000 cycles and 25 h of operation in acid. To understand the high activity of the *x* = 0.6 composition, first-principles calculations were carried out for the (110) metal/B layers of *x* = 0.66 and 0.5. We discovered that this mixed layer promotes hydrogen

evolution more efficiently for  $x = 0.66$  than for  $x = 0.5$ . In fact, we found that at all H coverages (20–100%),  $\Delta G_{\text{H}}$  reaches zero between 85 and 90% H coverage for  $x = 0.66$  while it never reaches zero for  $x = 0.5$ , indicating that the (110) layer performs much better for  $x = 0.66$ , thus supporting the experimental results. Furthermore, for the above-mentioned  $\alpha\text{-Mo}_{0.6}\text{W}_{0.4}\text{B}_2$ , the  $\Delta G_{\text{H}}$  plot for the (110) surface crossed zero below 60%, a much smaller percentage than that of  $\alpha\text{-Cr}_{0.33}\text{Mo}_{0.66}\text{B}_2$ , indicating better performance of the latter at high H coverages.<sup>3</sup> This result corroborates the experimental findings of a much smaller overpotential at 150 mA/cm<sup>2</sup> current density for the Cr-based phase (cf. Figures 4 and 6). In addition, the best member of the solid solution,  $\alpha\text{-Cr}_{0.4}\text{Mo}_{0.6}\text{B}_2$ , was found to outperform Pt/C at very high current densities (Figure 6, right) because it needs 180 mV less overpotential to drive an 800 mA/cm<sup>2</sup> current density.<sup>3</sup> This discovery paves the way for the realization of the potential of nonprecious MBs as suitable candidates to replace Pt/C.

### MBs with Boron Chain Substructures: Leveraging Boron Chain Condensation in HER

As shown above, monoborides containing zigzag single chains of boron atoms such as  $\alpha\text{-MoB}$  and  $\beta\text{-MoB}$  are as competitive toward HER as diborides containing layers of boron atoms. Therefore, the extraordinarily rich crystal chemistry of MBs allows for an exploration of the effect of boron substructure variations on the HER activity of these materials. For example, in the V–B system, several phases exist between the monoboride VB and the diboride VB<sub>2</sub>, namely, V<sub>5</sub>B<sub>6</sub> (space group *Cmcm*), V<sub>3</sub>B<sub>4</sub> (Cr<sub>3</sub>B<sub>4</sub>-type structure, *Immm*), and V<sub>2</sub>B<sub>3</sub> (*Cmcm*). Interestingly, we recently found that V<sub>3</sub>B<sub>4</sub>, the structure of which contains double boron chains (or chain of hexagons, Figure 7), has a lower overpotential than VB but a higher overpotential than VB<sub>2</sub>, a discovery that suggested a relationship between HER activity and boron chain condensation in V<sub>x</sub>B<sub>y</sub> phases.<sup>4</sup> Indeed, using the idea of boron chain condensation from one chain to a double chain to infinite chains (boron layer), we could derive an exponential equation (eq 1) that helped not only to predict the overpotential of all known V<sub>x</sub>B<sub>y</sub> phases but also to predict unknown phases (e.g., V<sub>5</sub>B<sub>8</sub> with four condensed boron chains, Figure 7), their crystal structures, and their overpotentials.

$$\eta(\text{mV}) = -90e^{-0.25n} - 205 \quad (1)$$

In eq 1,  $\eta$  is the overpotential at  $-10 \text{ mA/cm}^2$  current density and  $n$  (1, 2... $\infty$ ) is the ratio of the number of three-bonded boron atoms to that of two-bonded boron atoms in the unit cell of a given vanadium boride. Interestingly, eq 1 can also be used to predict the overpotentials of hybrid structures (i.e., structures containing a combination of different boron chains). For example, the overpotential of the known hybrid V<sub>5</sub>B<sub>6</sub> ( $n = 1.5$ ) is predicted to be between that of VB and V<sub>3</sub>B<sub>4</sub> because its structure contains 50% single boron chains and 50% double boron chains. This finding also hints at potentially unknown hybrid structures ( $n = 2.5, 3.5...$ ) with competitive HER activities. As we have seen for the diborides above, the HER activity of all of these boron-chain-based MBs can be further improved by solid solution formation, and such studies are in progress.

## ■ UNDERSTANDING THE HER ACTIVITY OF NONPRECIOUS BULK METAL BORIDES

Per definition, an active electrocatalyst should have high electrical conductivity, thus making all metallic systems potentially interesting candidates. However, their activity will further depend on their ability to moderately (not too tightly and not too loosely) bind atomic hydrogen on their surfaces. As mentioned in the Introduction, MBs can be divided into three groups depending on the metal-to-boron ratio (M/B): metal-rich borides (M/B > 2), boron-rich borides (M/B < 2), and borides with intermediate boron content. The electrical conductivity of the boron-rich borides usually varies from poorly conductive to semiconductive, making them unattractive electrocatalysts.<sup>5,6</sup> Metal-rich borides are highly conductive, and they can be attractive electrocatalysts if the metal is precious (e.g., Ru<sub>7</sub>B<sub>3</sub>).<sup>21</sup> If nonprecious metals are used, then their HER activity is noncompetitive due to the dominant amount of the nonprecious metals.<sup>27,30</sup> However, increasing the number of boron atoms in these metal-rich nonprecious MBs changes their electronic structures, thus leading to a significant downshift of the metal's d-band center compared to that of the pure metal.<sup>32</sup> This method has proven to be effective in predicting the HER activity of electrocatalysts in general. While the method explains the overall electrocatalytic behavior, the actual catalytic activity is surface-dependent, so the surface termination is crucial. Therefore, for a bulk electrocatalyst to be efficient, several of the exposed surfaces must be active to maximize the activity of these low-surface-area materials. Consequently, the distinct HER activities of different potentially exposed surfaces of the bulk electrocatalyst have been investigated via calculations of  $\Delta G_{\text{H}}$ . For example, high-resolution transmission electron microscopy (HRTEM) identified several surfaces on the MB<sub>2</sub> (M = Mo, V) particles: (001), (100), (110), and (101). Different terminations of these surfaces were then investigated via  $\Delta G_{\text{H}}$  calculations at various H coverages. It was found (see Figure 2, solid lines), at 25% H coverage, that  $\Delta G_{\text{H}}$  for mixed M/B-terminated (110) and (101) surfaces and B-terminated (001) and V-terminated (100) surfaces indicates better HER activities than for the M-terminated (001) and the Mo- and B-terminated (100) surfaces.<sup>22</sup> It should be noted that all active surfaces have free energies comparable to that of noble metal Pt (Figure 2), thus underscoring their high HER activity at 25% H coverage. However, to fully understand the HER activity it is important to examine the behavior of  $\Delta G_{\text{H}}$  as a function of H coverage since the high-percentage H coverage can be related to the behavior of the catalyst at high current density. In general,  $\Delta G_{\text{H}}$  increases with increasing H coverage for all surfaces except for the Mo-terminated (100) surface, in which  $\Delta G_{\text{H}}$  slightly decreases. Also, at higher H coverages, the (101) surface of MoB<sub>2</sub> becomes far less active at 100% H coverage. On the basis of these findings, the two binary bulk borides should have very competitive and similar HER activities.<sup>22,28</sup> Evidently, their high activity in the bulk can be explained by the large number of active surfaces. Nevertheless, the activity of these MBs can be further improved by using nanomaterials instead of bulk samples.



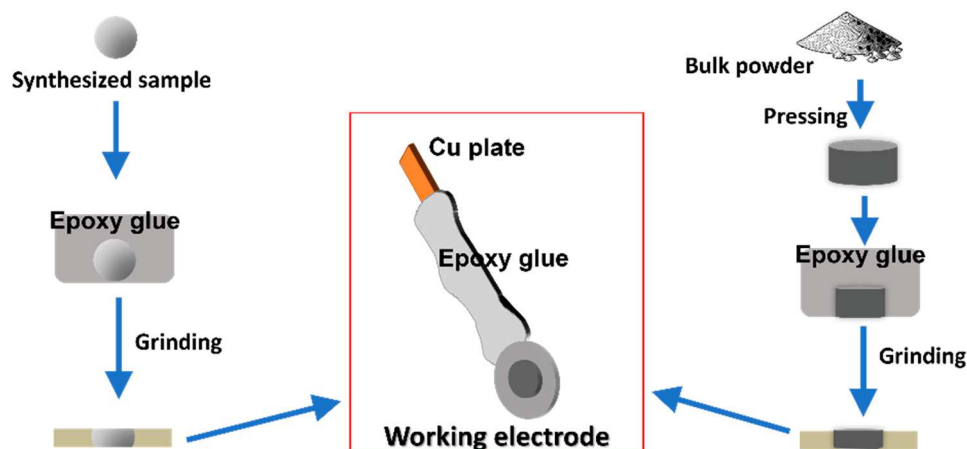


Figure 8. Electrode preparation process for bulk materials

### ■ CRYSTALLINE NANOMATERIALS OF NONPRECIOUS MBS FOR IMPROVED HER ACTIVITY

Most nanomaterials such as transition-metal carbides, phosphides, nitrides, and chalcogenides have been extensively studied for their various properties in recent years. However, transition-metal borides have seen little interest from the chemistry and materials science communities, mainly because single-phase and highly dispersed nanocrystalline MBs are notoriously difficult to synthesize. Therefore, the search for new synthesis strategies toward single-phase nanocrystalline MBs remains a hot topic. Many synthesis methods have been recently attempted, such as metal flux synthesis (Al and Sn), wet-chemical synthesis, borohydride reduction, an inorganic molten salt approach, and solid-state metathesis based on  $\text{MgB}_2$ .<sup>25</sup> Recently, we discovered a simple, general synthesis method for crystalline MBs nanomaterials.<sup>33</sup> This new method takes advantage of the redox chemistry of Sn/ $\text{SnCl}_2$ , the volatility and recrystallization of  $\text{SnCl}_2$  under the synthesis conditions, and the immiscibility of tin with boron to produce nanocrystalline MBs of 3d, 4d, and 5d transition metals. While numerous shapes of nanoborides can be synthesized by all of these synthetic methods, the use of high temperatures (700–900 °C) always lead to highly agglomerated particles. In fact, this issue remains the most important puzzle to be solved to boost the adoption of borides in many nanoscale applications including electrocatalysis. Despite this disadvantage, we recently showed that even agglomerated nanoborides outperform their bulk counterparts when studied under the same conditions. For example, the HER overpotentials of agglomerated  $\text{MoB}_2$  and  $\text{VB}_2$  nanoparticles have been improved by ca. 150 mV if compared with those found for their bulk under the same conditions.<sup>22,28</sup> This improved HER activity is due to the increased surface area and higher density of active sites, which can be proven by ECSA measurements (via  $C_{\text{dl}}$  values).  $\text{MoB}_2$  and  $\text{VB}_2$  nanoparticles have significantly higher  $C_{\text{dl}}$  values (27.8  $\text{mF}/\text{cm}^2$  for  $\text{MoB}_2$  and 8.1  $\text{mF}/\text{cm}^2$  for  $\text{VB}_2$ ) than their respective bulk particles. Furthermore, the two nanocatalysts yield Tafel slopes of 49 and 68 mV/dec, which are much smaller than those of bulk samples ( $\sim 126$  mV/dec), thus indicating an increase in the HER rate with decreasing particle size.

### ■ ELECTRODE PREPARATION OF BULK VERSUS NANOMATERIALS

Electrode preparation is very important to accurately assess the activity of materials. This is because a preparation method affects the electrochemical performance, and the activity of the studied material can be maximized. For instance, drop-cast bulk  $\alpha\text{-MoB}_2$  showed an overpotential of 300 mV for HER to drive 10  $\text{mA}/\text{cm}^2$  ( $\eta_{10} = 300$  mV). However, an  $\alpha\text{-MoB}_2$  disk-type electrode prepared by cutting and polishing an arc-melted sample required 74 mV less overpotential to achieve the same current density ( $\eta_{10} = 226$  mV).<sup>30</sup> Moreover, the activity of the pressed disk-type electrode, which was synthesized at high pressure, was improved 2-fold ( $\eta_{10} = 149$  mV) compared to that of the drop-casted electrode even though it is the same  $\alpha\text{-MoB}_2$  phase.<sup>34</sup> The lower activity of drop-casted bulk electrodes comes from the inefficient surface coverage of the electrode. While the disk-type electrode surface is completely covered, that of the drop-casted electrode cannot be covered completely because the particle size of the bulk powder is too large to be dispersed in the solution. This difference can lead to the misinterpretation of the intrinsic activity. Therefore, to evaluate the catalytic performance precisely, it is very important to apply the appropriate electrode preparation method according to the type of material. The most common electrode preparation method is drop-casting, which is suitable for nanomaterials but unsuitable for bulk samples. Typically, a drop-casting electrode is prepared by dispersing 1 mg of catalyst in 95  $\mu\text{L}$  of isopropanol (or ethanol) and 5  $\mu\text{L}$  of Nafion. Then the catalyst mixture is coated dropwise on a carbon cloth or glassy carbon to achieve a catalyst loading of approximately 0.3–0.5  $\text{mg}/\text{cm}^2$ , followed by drying for 5 h at 50 °C. This method, which relies on the homogeneous dispersion of the solid catalyst in solution to cover the holistic electrode surface, is proper for a nanosized powder. On the contrary, for bulk materials, such as arc-melted spherical samples or pressed pellets of powder samples, a dense disk-shaped sample can be directly used as an electrode. As shown in Figure 8, a dense synthesized sample or pressed bulk powder is put into an epoxy glue and dried overnight at room temperature. Then, the top and bottom of the dried sample are polished, followed by attaching it to a copper plate using conductive silver paste. The exposed surface of the copper plate is covered with epoxy adhesive and dried overnight at

room temperature. This method is proper for bulk materials because the whole electrode surface is covered by the catalyst.

## CONCLUSIONS AND PERSPECTIVES

In this Account, we have demonstrated how experimental and computational methods can be effectively used to understand and predict new nonprecious MB HER electrocatalysts. We focused on the importance of boron and its substructures in achieving extraordinary HER performances and the importance of using structure–activity relationships to design next-generation electrocatalysts. Studies of the Mo–B system have shown that the diboride MBs are the most active; however, those containing the flat graphene-like boron layers are more active than those with puckered phosphorene-like layers. Density functional theory (DFT) calculations have shown that the (001) boron layer in hexagonal diborides MB<sub>2</sub> (h-MoB<sub>2</sub>) is the most active surface and has an HER activity behavior similar to that of the benchmark Pt(111) surface. However, free-energy calculations have also shown that several layers are active in these materials, thus explaining their high activity in the bulk. In the V–B system, these findings were confirmed and extended to the discovery of the boron chain dependence of the HER activity in MBs. In fact, as the boron chains are condensed from single to double all the way to infinite (layer), the HER activity incrementally increases, leading to an accurate mathematical prediction of the HER activity of unknown MBs and their crystal structures. Moreover, lowering the particle size of these MBs leads to a significant improvement of their activity from their bulk counterparts. However, strong particle agglomeration still hinders the fulfillment of their full potential, thus future work should focus on the synthesis of highly dispersed MBs. Finally, the electrode preparation must be done properly to maximize the activity of MBs, especially in cases of bulk samples where traditional drop-casting is ineffective due to the inefficient surface coverage, thus densified disk-shaped electrodes are more suitable.

## AUTHOR INFORMATION

### Corresponding Author

**Boniface P. T. Fokwa** – Departments of Chemistry and Chemical and Environmental Engineering, Center for Catalysis, University of California, Riverside, Riverside, California 92521, United States; [orcid.org/0000-0001-9802-7815](https://orcid.org/0000-0001-9802-7815); Email: [bfokwa@ucr.edu](mailto:bfokwa@ucr.edu), [fokwalab.ucr.edu](http://fokwalab.ucr.edu)

### Author

**Eunsoo Lee** – Departments of Chemistry and Chemical and Environmental Engineering, Center for Catalysis, University of California, Riverside, Riverside, California 92521, United States

Complete contact information is available at:

<https://pubs.acs.org/10.1021/acs.accounts.1c00543>

### Notes

The authors declare no competing financial interest.

### Biographies

**Eunsoo Lee** received his B.S. and M.S. from Inha University (South Korea) and joined the Fokwa group at the University of California, Riverside in 2017. His main research interests are the synthesis,

physicochemical properties, and electrocatalytic activity studies of intermetallic compounds.

**Boniface P. T. Fokwa** obtained his B.S. and M.S. from the University of Yaounde I (Cameroon), his Ph.D. from Dresden University of Technology (Germany), and his Habilitation from RWTH Aachen University (Germany). After working as a Heisenberg Fellow at RWTH, he moved to the University of California, Riverside in 2015 and currently holds the position of full professor. His research group combines experimental and computational methods to rationally design materials for energy-related applications such as magnetic, battery, and electrocatalytic materials.

## ACKNOWLEDGMENTS

The authors thank the National Science Foundation (Career Award to B.P.T.F., no. DMR-1654780) and UC Riverside (startup funds to B.P.T.F.) for financial support. We thank all actual and former Fokwa group members and all collaborators for their contributions to the success of this research.

## REFERENCES

- (1) Park, H.; Encinas, A.; Scheifers, J. P.; Zhang, Y.; Fokwa, B. P. T. Boron-dependency of molybdenum boride electrocatalysts for the hydrogen evolution reaction. *Angew. Chem., Int. Ed.* **2017**, *56*, 5575–5578.
- (2) Park, H.; Zhang, Y.; Scheifers, J. P.; Jothi, P. R.; Encinas, A.; Fokwa, B. P. T. Graphene-and phosphorene-like boron layers with contrasting activities in highly active Mo<sub>2</sub>B<sub>4</sub> for hydrogen evolution. *J. Am. Chem. Soc.* **2017**, *139*, 12915–12918.
- (3) Park, H.; Lee, E.; Lei, M.; Joo, H.; Coh, S.; Fokwa, B. P. T. Canonic-Like HER Activity of Cr<sub>1-x</sub>MoxB<sub>2</sub> Solid Solution: Overpowering Pt/C at High Current Density. *Adv. Mater.* **2020**, *32*, 2000855.
- (4) Lee, E.; Park, H.; Joo, H.; Fokwa, B. P. T. Unexpected Correlation Between Boron Chain Condensation and HER Activity in Highly Active Vanadium Borides: Enabling Predictions. *Angew. Chem., Int. Ed.* **2020**, *59*, 11774–11778.
- (5) Fokwa, B. P. T. Borides: Solid-State Chemistry. *Encyclopedia of Inorganic and Bioinorganic Chemistry* **2014**, 1–14.
- (6) Akopov, G.; Yeung, M. T.; Kaner, R. B. Rediscovering the crystal chemistry of borides. *Adv. Mater.* **2017**, *29*, 1604506.
- (7) Albert, B.; Hillebrecht, H. Boron: elementary challenge for experimenters and theoreticians. *Angew. Chem., Int. Ed.* **2009**, *48*, 8640–8668.
- (8) Dinh, K. N.; Liang, Q.; Du, C.-F.; Zhao, J.; Tok, A. I. Y.; Mao, H.; Yan, Q. Nanostructured metallic transition metal carbides, nitrides, phosphides, and borides for energy storage and conversion. *Nano Today* **2019**, *25*, 99–121.
- (9) Skrabalak, S. E.; Suslick, K. S. On the possibility of metal borides for hydrodesulfurization. *Chem. Mater.* **2006**, *18*, 3103–3107.
- (10) Gao, X.-P.; Yang, H.-X. Multi-electron reaction materials for high energy density batteries. *Energy Environ. Sci.* **2010**, *3*, 174–189.
- (11) Ha, M.-A.; Baxter, E. T.; Cass, A. C.; Anderson, S. L.; Alexandrova, A. N. Boron switch for selectivity of catalytic dehydrogenation on size-selected Pt clusters on Al<sub>2</sub>O<sub>3</sub>. *J. Am. Chem. Soc.* **2017**, *139*, 11568–11575.
- (12) Grant, J. T.; McDermott, W. P.; Venegas, J. M.; Burt, S. P.; Micka, J.; Phivilay, S. P.; Carrero, C. A.; Hermans, I. Boron and boron-containing catalysts for the oxidative dehydrogenation of propane. *ChemCatChem* **2017**, *9*, 3623–3626.
- (13) Qin, G.; Cui, Q.; Du, A.; Wang, W.; Sun, Q. Transition metal diborides: A new type of high-performance electrocatalysts for nitrogen reduction. *ChemCatChem* **2019**, *11*, 2624–2633.
- (14) Gupta, S.; Patel, M. K.; Miotello, A.; Patel, N. Metal boride-based catalysts for electrochemical water-splitting: A review. *Adv. Funct. Mater.* **2020**, *30*, 1906481.



- (15) Chen, Z.; Duan, X.; Wei, W.; Wang, S.; Zhang, Z.; Ni, B.-J. Boride-based electrocatalysts: Emerging candidates for water splitting. *Nano Res.* **2020**, *13*, 293–314.
- (16) Chen, H.; Zou, X. Intermetallic borides: structures, synthesis and applications in electrocatalysis. *Inorg. Chem. Front.* **2020**, *7*, 2248–2264.
- (17) Pei, Y.; Zhou, G.; Luan, N.; Zong, B.; Qiao, M.; Tao, F. F. Synthesis and catalysis of chemically reduced metal-metalloid amorphous alloys. *Chem. Soc. Rev.* **2012**, *41*, 8140–8162.
- (18) Masa, J.; Weide, P.; Peeters, D.; Sinev, I.; Xia, W.; Sun, Z.; Somsen, C.; Muhler, M.; Schuhmann, W. Amorphous cobalt boride (Co<sub>2</sub>B) as a highly efficient nonprecious catalyst for electrochemical water splitting: oxygen and hydrogen evolution. *Adv. Energy Mater.* **2016**, *6*, 1502313.
- (19) Gupta, S.; Patel, N.; Miotello, A.; Kothari, D. Cobalt-boride: An efficient and robust electrocatalyst for hydrogen evolution reaction. *J. Power Sources* **2015**, *279*, 620–625.
- (20) Li, H.; Wen, P.; Li, Q.; Dun, C.; Xing, J.; Lu, C.; Adhikari, S.; Jiang, L.; Carroll, D. L.; Geyer, S. M. Earth-abundant iron diboride (FeB<sub>2</sub>) nanoparticles as highly active bifunctional electrocatalysts for overall water splitting. *Adv. Energy Mater.* **2017**, *7*, 1700513.
- (21) Zou, X.; Wang, L.; Ai, X.; Chen, H.; Zou, X. Crystal phase-dependent electrocatalytic hydrogen evolution performance of ruthenium-boron intermetallics. *Chem. Commun.* **2020**, *56*, 3061–3064.
- (22) Jothi, P. R.; Zhang, Y.; Yubuta, K.; Culver, D.; Conley, M.; Fokwa, B. Abundant vanadium diboride with graphene-like boron layers for hydrogen evolution. *ACS Appl. Energy Mater.* **2019**, *2*, 176–181.
- (23) Li, Q.; Zou, X.; Ai, X.; Chen, H.; Sun, L.; Zou, X. Revealing activity trends of metal diborides toward pH-universal hydrogen evolution electrocatalysts with Pt-like activity. *Adv. Energy Mater.* **2018**, *9*, 1803369.
- (24) Zhu, J.; Hu, L.; Zhao, P.; Lee, L. Y. S.; Wong, K.-Y. Recent advances in electrocatalytic hydrogen evolution using nanoparticles. *Chem. Rev.* **2020**, *120*, 851–918.
- (25) Carenco, S.; Portehault, D.; Boissiere, C.; Mezailles, N.; Sanchez, C. Nanoscaled metal borides and phosphides: recent developments and perspectives. *Chem. Rev.* **2013**, *113*, 7981–8065.
- (26) Vrubel, H.; Hu, X. Molybdenum boride and carbide catalyze hydrogen evolution in both acidic and basic solutions. *Angew. Chem., Int. Ed.* **2012**, *51*, 12703–12706.
- (27) Li, Q.; Wang, L.; Ai, X.; Chen, H.; Zou, J.; Li, G.-D.; Zou, X. Multiple crystal phases of intermetallic tungsten borides and phase-dependent electrocatalytic property for hydrogen evolution. *Chem. Commun.* **2020**, *56*, 13983–13986.
- (28) Jothi, P. R.; Zhang, Y.; Scheifers, J. P.; Park, H.; Fokwa, B. P. T. Molybdenum diboride nanoparticles as a highly efficient electrocatalyst for the hydrogen evolution reaction. *Sustain. Energy Fuels* **2017**, *1*, 1928–1934.
- (29) Tang, Q.; Jiang, D.-E. Mechanism of hydrogen evolution reaction on 1T-MoS<sub>2</sub> from first principles. *ACS Catal.* **2016**, *6*, 4953–4961.
- (30) Park, H.; Zhang, Y.; Lee, E.; Shankari, P.; Fokwa, B. P. T. High-Current-Density HER Electrocatalysts: Graphene-like Boron Layer and Tungsten as Key Ingredients in Metal Diborides. *ChemSusChem* **2019**, *12*, 3726–3731.
- (31) Wang, J.; Xu, F.; Jin, H.; Chen, Y.; Wang, Y. Non-noble metal-based carbon composites in hydrogen evolution reaction: fundamentals to applications. *Adv. Mater.* **2017**, *29*, 1605838.
- (32) Ai, X.; Zou, X.; Chen, H.; Su, Y.; Feng, X.; Li, Q.; Liu, Y.; Zhang, Y.; Zou, X. Transition-Metal-Boron Intermetallics with Strong Interatomic d-sp Orbital Hybridization for High-Performance Electrocatalysis. *Angew. Chem., Int. Ed.* **2020**, *59*, 3961–3965.
- (33) Jothi, P. R.; Yubuta, K.; Fokwa, B. P. A simple, general synthetic route toward nanoscale transition metal borides. *Adv. Mater.* **2018**, *30*, 1704181.
- (34) Chen, Y.; Yu, G.; Chen, W.; Liu, Y.; Li, G.-D.; Zhu, P.; Tao, Q.; Li, Q.; Liu, J.; Shen, X. Highly active, nonprecious electrocatalyst comprising borophene subunits for the hydrogen evolution reaction. *J. Am. Chem. Soc.* **2017**, *139*, 12370–12373.



ACS IN FOCUS

Cellu  
Agricu  
Lab-Grown  
Dilek Erilli-C  
Dorothee E

Machine  
Learning in  
Chemistry  
Jon Paul Janet &  
Heather J. Kulik

bacterials  
Loria Cheng Jaramillo  
William M. Wuest

ACS In Focus ebooks are digital publications that help readers of all levels accelerate their fundamental understanding of emerging topics and techniques from across the sciences.

pubs.acs.org/series/infocus

ACS Publications  
Most Trusted. Most Cited. Most Read.

QR code